

The structure and kinematics of the the Galaxy thin gaseous disc outside the solar orbit ¹

G. Galazutdinov^{1,2}

¹ *Instituto de Astronomia, Universidad Catolica del Norte, Av. Angamos 0610, Antofagasta, Chile*

² *Pulkovo Observatory, Pulkovskoe Shosse 65, Saint-Petersburg 196140, Russia*

runizag@gmail.com

A. Strobel

Center for Astronomy, Nicholas Copernicus University, Gagarina 11, Pl-87-100 Toruń, Poland

astrobel@astri.umk.pl

F.A.Musaev^{3,4,5}

³ *Special Astrophysical Observatory of the Russian AS, Nizhnij Arkhyz 369167, Russia*

⁴ *Institute of Astronomy of the Russian AS, 48 Pyatnitskaya st., 119017 Moscow, Russia*

⁵ *Terskol Branch of Institute of Astronomy of the Russian AS, 361605 Peak Terskol, Kabardino-Balkaria, Russia*

faig@sao.ru

A. Bondar

ICAMER, Peak Terskol, Kabardino-Balkaria, 361605, Russia

arctur.ab@gmail.com

and

J. Krelowski

Center for Astronomy, Nicholas Copernicus University, Gagarina 11, Pl-87-100 Toruń, Poland

jacek@astri.umk.pl

ABSTRACT

The rotation curve of the Galaxy is generally thought to be flat. However, using radial velocities from interstellar molecular clouds, which is common in rotation curve determination, seems to be incorrect and may lead to incorrectly inferring that the

rotation curve is flat indeed. Tests basing on photometric and spectral observations of bright stars may be misleading. The rotation tracers (OB stars) are affected by motions around local gravity centers and pulsation effects seen in such early type objects. To get rid of the latter a lot of observing work must be involved. We introduce a method of studying the kinematics of the thin disc of our Galaxy outside the solar orbit in a way that avoids these problems. We propose a test based on observations of interstellar CaII H and K lines that determines both radial velocities and distances. We implemented the test using stellar spectra of thin disc stars at galactic longitudes of 135° and 180° . Using this method, we constructed the rotation curve of the thin disc of the Galaxy. The test leads to the obvious conclusion that the rotation curve of the thin gaseous galactic disk, represented by the CaII lines, is Keplerian outside the solar orbit rather than flat.

Subject headings: ISM: atoms – kinematics and dynamics – lines and bands

1. Introduction

It is very likely that our Galaxy is a spiral barred galaxy, i.e. its nucleus is surrounded by a bar. The dominant component at the location of the Sun is the thin disc, composed of young stars and interstellar clouds, of which the Sun is a tiny part. The interior of the Galaxy is dominated by the bulge/bar, while further out the dominant component is believed to be the dark halo, probably consisting of dark matter (DM), about which we know very little. The dark halo is especially problematic for a Galaxy modeler because it can so far only be detected through its gravitational field. Dark matter is thought to be made up of a one or more types of elementary particles that have not been detected on the Earth. The properties of these particles can only be speculated about, so it is hard to design an experiment to detect them. A major goal of a Galaxy modeler is to make a map of the gravitational field of the dark halo from observations. (The mass distribution of the dark halo can be inferred from the gravitational field that it generates.) The difference between the gravitational field of the whole Galaxy and the combined fields of the visible components yields the field of the dark halo.

Over the last few years a sustained effort has been made to interpret observations of the kinematics of interstellar gas, based on the assumption that HI, HII and H₂ clouds move on closed orbits, usually assumed to be circular. These clouds are considered as tracers of the gaseous thin disc. Visual inspection of UV and visual pictures of galaxies, situated edge-on, shows that the cold, likely evolved objects, are distributed in a different way than the dense interstellar matter and OB

¹This paper includes data gathered with the 2 m telescope at the ICAMER Observatory (Terskol, Russia) and the 1.8 m telescope at Bohyunsan Optical Astronomy Observatory (South Korea).

stars that form thin galactic discs. However, the case of HI clouds, being revealed by the 21 cm spectral feature, is not that certain. It is evident that galaxies were formed out of neutral hydrogen but other abundant elements have been formed inside galaxies.

Molecular clouds and ionized hydrogen clouds are more likely to be spatially correlated with the thin disc since OB stars, which excite HII clouds and are used to measure their distances, are recently formed out of dense, molecular, interstellar clouds. However, molecular spectral features seen in spectra of OB stars might be formed not in the remnants of HII region parent clouds but “somewhere” along the sightlines to the latter.

The existence of dark matter in and around spiral galaxies (like our own Milky Way) is indirectly, dynamically indicated by the nearly flat rotation curves in the outer parts of these galaxies that are constructed under the assumption of circular rotation of the tracers—see e.g. Sofue & Rubin (2001). This approximately constant speed of galactic rotation, independent of the distance from the galaxy centers, is usually considered to provide rigorous proof of the presence of DM around our and other galaxies. The analysis of stellar motions by Kuijken & Gilmore (1989), Holmberg, & Flynn, (2000) provide no strong evidence for dark matter, while not ruling it out either. These analyzes were based on the motions of quite nearby stars. This is because the density of galactic objects declines outside the solar orbit, making it difficult to construct statistically significant samples of tracers situated outside the solar circle. The main source of information used for construction of the Galactic disc rotation curve is the velocities of CO clouds, which are believed to be spatially correlated with HII regions, but there have been attempts to apply other tracers. Since the 1970s, the distances used are those based on the distances of very bright objects, such as OB stars and their clusters. The radial velocities are measured either using H_α lines originating in HII regions (Georgelin & Georgelin 1976) or using (usually) CO lines in molecular clouds (Clemens 1985). Moffat, Jackson & Fitzgerald (1979) tried to improve the distance measurements using a zero-age main sequence (ZAMS) fitting method for HII regions, but distances to these objects that are normally used are those based on spectroscopic parallax. Moreover, it is assumed that HII regions and molecular clouds are at the same distances as the stars observed. This is likely to be true in the case of HII regions, but these regions are expanding shells of ionized gas and thus a great scatter in velocities is to be expected. Interstellar molecular lines observed in the spectra of OB stars may originate in clouds along the sightline, but at large distances from the observed stars.

Maciel and Lago (2005) compared the Galactic rotation curve based on a large sample of planetary nebulae with that of Brand and Blitz (1993) based on HII regions. Planetary-nebulae-derived rotation velocities are systematically lower than those for HII regions. This may be either due to uncertainties of distance measurements or due to different kinematics of HII regions and planetary nebulae.

Several articles present Galaxy rotation curves based on stellar spectrophotometry. Liu & Zhu (2010) used 194 carbon stars at distances up to $R=15$ kpc from the Galactic centre and reported a flat rotation curve with considerable scatter. A similar result was recently reported by López-

Corredera (2014), who derived the rotation curve of the Galaxy in the range of Galactocentric radii $R=4\text{--}16$ kpc using the proper motions of red clump giants and near-infrared photometric data from the 2MASS survey. A flat rotation curve for the outer Galaxy, based on radial velocities of red giants and horizontal branch stars was also obtained by Xue et al. (2008) and by Bovy et al. (2012).

Discrepancies between the galactic rotation curve and a Keplerian one are usually interpreted either in terms of DM or MOND (Modified Newtonian Dynamics), see e.g. Milgrom (1983). Recent determinations of the rotation curve of M31 based on the observations of its gaseous disk, even show a rise of the speed of rotation in its outer parts, which cannot be understood in terms of standard DM models or perturbations of the M31’s disk by its satellites (Chemin et al. (2009), Corbelli et al., 2010).

Quite recently, strong support for the flatness of the outer Galactic rotation curve seems to be provided by very precise astrometric measurements made as part of the VERA program of trigonometric parallaxes and proper motions of a few star-forming regions distributed far away beyond the solar orbit: Toshihiro et al. (2009), Reid et al. (2009); Oh et al. (2010). These results favor a nearly flat, or even slightly rising outward Galactic rotation speed up to 13 kpc from the Galactic center and indicate that this curve is similar to that of the Andromeda Galaxy.

Sofue et al. (2009) have unified the existing data on the rotation curve of the Galaxy, presenting a single rotation curve by re-calculating distances and velocities, adopting for the galactocentric distance and the orbital velocity of the Sun the values $(R_{\odot}, V_{\odot})=(8.0 \text{ kpc}, 200 \text{ km/s})$. The resulting curve is generally flat, but two local minima, or dips, are prominent: at the radii 3 and 9 kpc. The 3-kpc dip is consistent with the observed bar (or alternatively explained by a massive ring with the density maximum at a radius of 4-kpc). The 9-kpc dip is clearly exhibited by different tracers as the most peculiar feature in the Galactic rotation curve. The authors explain it by a massive ring with the density peak at a radius of 11-kpc. This great ring may be related to the Perseus arm. It is evident that the sample of tracers situated outside the solar orbit (and believed to be intrinsically related to the Galaxy) is much smaller than that of inner tracers. Moreover, the scatter

Table 1: Data on the clusters taken from the Simbad database. Radial velocity values are rounded. Galactic coordinates l, b and the number of stars N used for calculating the mean RV value are listed.

Cluster	l	b	dist (pc)	RV_{\odot} (km/s)	N	Ref.
NGC 884	135.1	-3.6	2940	-43 ± 1	5	Dias et al. (2002)
NGC 869	134.6	-3.7	2079	-42 ± 2	54	Kharchenko et al. (2005a)
ASCC 4	123.1	-1.3	750	-9 ± 9	4	Kharchenko et al. (2005b)
Stock 2	133.3	-1.7	303	2 ± 2	27	Kharchenko et al. (2005a)
IC 1848	137.2	0.9	2002	-47 ± 7	4	Dias et al. (2002)
IC 1805	134.7	0.9	2344	-45 ± 11	6	Dias et al. (2002)

Table 2: Data on the observed stars (Northern hemisphere) and equivalent width of CaII K and H lines. RV_{\odot} - heliocentric radial velocity of the star. V_{rot} - calculated orbital velocity. t- Terskol, b-BOES

Star	l	b	EW(K) (mÅ)	EW(H) (mÅ)	dist (pc)	RV_{\odot} (km/s)	V_{rot} (km/s)	R_{gc} (kpc)
+56-574t	135.0	-03.6	458±32	266±25	1700 ⁺⁶⁵⁰ ₋₄₀₀	-42	176	9.3
+59-451b	133.4	-1.4	432±18	294±22	2317 ⁺³⁰⁸ ₋₂₈₅	-50	173	9.7
+59-456b	133.7	-1.3	544±12	387±17	3277 ⁺²⁸⁸ ₋₂₇₀	-52	183	10.5
+60-470t	133.9	-0.1	453±28	339±27	3200 ⁺⁸⁰⁰ ₋₆₀₀	-44	197	10.5
+60-493b	134.6	0.6	551±10	377±10	2976 ⁺¹²¹ ₋₁₁₉	-43	194	10.3
+60-498t	134.6	+1.0	488±26	330±26	2600 ⁺¹⁰⁰⁰ ₋₆₀₀	-43	188	10.9
+60-499t	134.6	+1.0	562±63	343±57	2300 ⁺¹²⁰⁰ ₋₈₀₀	-51	170	9.8
+60-501t	134.7	+0.9	525±30	361±21	2900 ⁺¹⁰⁰⁰ ₋₆₀₀	-43	193	10.2
+60-513t	134.9	0.9	586±53	415±61	3478 ⁺⁵³⁸ ₋₈₁₂	-49	190	10.7
+60-526t	135.5	0.8	598±34	390±29	2847 ⁺²⁸⁵ ₋₂₇₇	-47	184	10.2
+60-594b	137.4	2.1	432±6	292±5	2276 ⁺⁴⁹ ₋₅₀	-43	180	9.8
+61-411t	133.8	+1.2	492±61	388±68	4100 ⁺¹⁴⁰⁰ ₋₂₀₀₀	-57	186	11.2
+61-468t	135.6	+2.1	371±26	242±24	1800 ⁺⁹⁰⁰ ₋₅₀₀	-34	190	9.4
2905t	120.8	0.1	247±2	174±3	1489 ⁺⁴⁹ ₋₄₉	-27	214	8.9
5394t	123.6	-2.1	17±2.1	8±2.1	117 ⁺¹⁵ ₋₁₄	-5	207	8.1
12323t	132.9	-5.9	313±17	221±11	1878 ⁺⁷⁴ ₋₇₄	-42	180	9.4
13256b	132.6	-0.6	608±32	418±23	3319 ⁺¹⁹² ₋₁₉₂	-52	184	10.5
13267t	133.5	-3.6	717±13	431±10	2950 ⁺³⁸⁸ ₋₃₄₀	-58	168	10.3
13716t	134.0	-03.3	469±18	282±19	1850 ⁺⁴⁵⁰ ₋₃₀₀	-44	176	9.4
13758t	134.6	-03.3	483±25	338±27	2800 ⁺¹²⁰⁰ ₋₇₀₀	-40	197	10.2
13831t	134.5	-04.2	509±16	366±15	3200 ⁺⁷⁰⁰ ₋₅₀₀	-48	188	10.5
13841t	134.4	-03.9	585±11	363±22	2500 ⁺⁴⁰⁰ ₋₄₀₀	-41	190	9.9
13854t	134.4	-3.9	578±30	360±19	2467 ⁺¹³⁰ ₋₁₂₉	-50	174	9.9
13866t	134.5	-04.2	530±19	316±11	2050 ⁺²⁰⁰ ₋₂₀₀	-49	170	9.5
13890t	134.5	-04.2	520±13	353±13	2750 ⁺⁴⁵⁰ ₋₃₅₀	-47	184	10.1
13969t	134.5	-03.8	526±14	333±16	2350 ⁺⁴⁰⁰ ₋₃₀₀	-46	179	9.8
14014t	134.8	-04.6	561±19	387±15	3100 ⁺⁶⁰⁰ ₋₄₅₀	-52	179	10.4
14053t	134.6	-03.9	581±16	358±15	2400 ⁺⁴⁰⁰ ₋₃₀₀	-43	185	9.8
14134t	134.6	-3.7	693±14	377±8	2207 ⁺⁴⁷ ₋₄₈	-57	158	9.7
14143t	135.0	-4.0	648±8	340±5	1930 ⁺³¹ ₋₃₂	-47	171	9.5
14302t	135.1	-04.4	526±18	312±13	2000 ⁺³⁰⁰ ₋₂₀₀	-40	184	9.5
14357t	135.0	-03.9	543±18	347±17	2450 ⁺⁵⁰⁰ ₋₃₅₀	-51	172	9.9
14434t	135.1	-03.8	517±13	338±13	2500 ⁺³⁵⁰ ₋₉₀₀	-46	181	9.9
14442t	134.2	-1.3	520±35	375±32	3250 ⁺¹¹⁵⁰ ₋₉₅₀	-54	178	10.5
14443t	135.0	-03.6	477±20	269±12	1650 ⁺²⁵⁰ ₋₂₀₀	-43	174	9.2
14476t	135.0	-03.5	507±15	288±17	1800 ⁺³⁰⁰ ₋₃₀₀	-45	172	9.4
14818t	135.6	-3.9	560±30	296±16	1702 ⁺⁸⁸ ₋₈₉	-49	164	9.3
14947t	135	-1.7	451±26	335±23	3111 ⁺²⁸⁶ ₋₂₈₁	-61	163	10.4
15558t	134.7	0.9	476±15	330±13	2675 ⁺¹⁴¹ ₋₁₃₉	-41	193	10.1
15570t	134.8	0.9	464±19	350±16	3361 ⁺¹⁸⁸ ₋₁₈₆	-50	187	10.6
15629t	134.8	+1.0	463±20	352±17	3450 ⁺⁹⁵⁰ ₋₇₅₀	-55	179	10.7
15785b	135.3	0.2	537±28	337±19	2338 ⁺¹⁴² ₋₁₄₀	-45	180	9.8
16310t	136.4	-0.9	537±28	337±19	2152 ⁺³¹⁰ ₋₂₈₆	-46	175	9.7
16429t	135.7	1.1	472±17	307±16	2249 ⁺¹⁶⁹ ₋₁₆₅	-50	170	9.7
17505t	137.2	+0.9	456±15	331±14	2900 ⁺⁷⁰⁰ ₋₄₅₀	-46	186	10.3
17520t	137.2	+0.9	494±32	357±29	3100 ⁺¹⁴⁰⁰ ₋₈₅₀	-48	184	10.5
20336t	137.5	+7.1	32±2	18±2	195 ⁺²⁹ ₋₃₈	-3	210	8.1
25940t	153.7	-3	30±2	22±1.2	271 ⁺⁵ ₋₆	0.1	238	8.2
236960t	134.6	-1.5	553±46	427±48	4300 ⁺¹⁷⁰⁰ ₋₁₆₀₀	-66	191	11.4
27192t	152.8	0.6	95±6	48±3.3	330 ⁺¹⁹ ₋₁₉	-2	237	8.3

of individual determinations of distances and radial velocities grows in a stepwise manner outside the solar orbit (see Fig. 1). These uncertainties in the measured radial velocities look strange; they very likely are from measurements of very broad H_α lines originating in HII regions, which do not allow precise radial velocity determinations.

The sudden growth in the scatter of points situated outside the solar orbit, seen in Fig. 1, follows the use of different methods to determine distances and orbital velocities inside and outside the solar orbit. Inside the solar circle, the method of tangent points is typically used. The orbital velocity of the point (tangent point) is uniquely determined by the maximal radial velocity in a given direction. At this point the radius vector of the observed object R_{GC} is perpendicular to the sightline. This gives a right triangle, i.e. all the triangle’s sides and angles are determined—including the galactocentric distance of the object observed at the tangent point. The result is scaled to the assumed radius of the solar orbit. The method of tangent points cannot be applied outside the solar circle. Thus, the rotation curve of galactic peripherals depends critically on measurements of individual distances and radial velocities. Such methods are called “clear” if they apply direct distance and radial velocity measurements; otherwise models based on certain assumptions are applied to large samples of objects.

2. Distance determination problems and why CaII is better tracer

The resulting, generally flat, rotation curve is an average one. The same concerns the rotation curves of other galaxies. The distances to tracers, especially for the outer part of the Galaxy, are either based on angular sizes of HI clouds in the Galactic disk (Merrifield, 1992), or on spectroscopic parallaxes of OB stars (plus ZAMS fitting). The former require assumptions of their linear sizes and thus remain very uncertain. The latter suffer large errors because of the scarcity of OB stars within the range of detectable trigonometric parallaxes, making the calibrated M'_V s uncertain. Moreover, massive OB stars are frequently spectroscopic binaries or, in general, variables. The apparent and absolute magnitude in photometric equations should be measured and calibrated at the same phase. Such a calibration, i.e. for different phases of variability, has not been done for bright, OB stars. The estimated distances, both those based on linear sizes of HI clouds and those resulting from ZAMS fitting thus suffer large errors, which themselves are difficult to estimate. A clear example will be shown later. However, the very error bars of the data, around the average rotation curve beyond the solar circle (Fig. 1) is shown only for the orbital velocities! The errors of distances are not given in the homepage of Sofue ².

The distance errors have not been estimated. The observed scatter should indicate not only significant errors in the distance and radial velocity determinations of the tracers used, but also more complex intrinsic kinematics of the considered outer disk. Visual inspection of images of

²<http://www.ioa.s.u-tokyo.ac.jp/~sofue/>

Table 3: Data on the observed stars (Galactic anticentre) and equivalent width of CaII K and H lines. All spectra are from Terskol

Star	l	b	EW(K) (mÅ)	EW(H) (mÅ)	dist (pc)	RV _⊙ (km/s)
43818	188.5	+03.9	297±18	225±3	2300 ⁺⁴⁵⁰ ₋₄₀₀	+16
40111	184.0	+00.8	165±3	99±3	700 ⁺⁶⁵ ₋₅₀	+12
254755	189.1	+03.3	415±19	315±18	3100 ⁺¹³⁰⁰ ₋₇₅₀	+19
254699	188.3	+03.7	317±21	217±13	1750 ⁺¹⁰⁰⁰ ₋₄₀₀	+16
254042	187.6	+03.5	326±21	247±18	2400 ⁺¹⁵⁰⁰ ₋₇₀₀	+15
255055	188.7	+03.9	301±13	228±14	2350 ⁺⁸⁵⁰ ₋₆₅₀	+14
255134	188.7	+03.9	298±16	247±21	2200 phot sat	+15
251847	187.0	+01.6	286±17	200±20	1700 ⁺⁹⁵⁰ ₋₅₀₀	+15
250028	184.9	+00.8	246±11	188±12	1900 ⁺⁹⁰⁰ ₋₅₀₀	+14
255091	188.2	+04.1	303±18	210±13	1750 ⁺⁶⁰⁰ ₋₄₀₀	+16
255312	188.8	+04.1	282±17	209±18	1950 ⁺¹²⁰⁰ ₋₅₅₀	+13

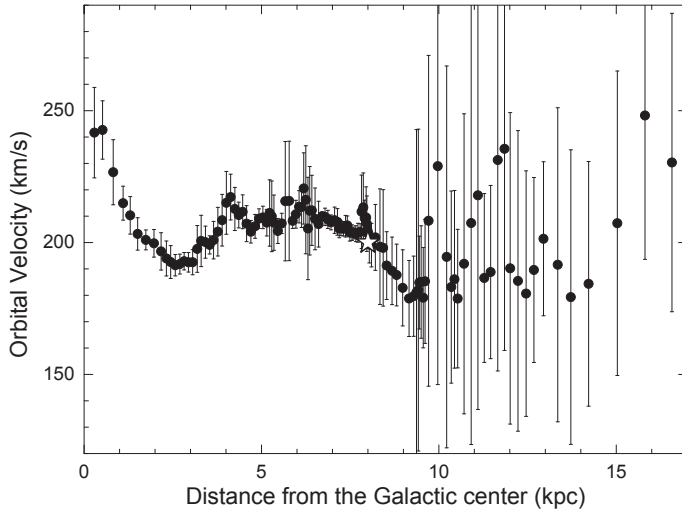


Fig. 1.— Average galactic rotation curve based on data from the Sofue’s web page. The position of the Sun is marked as ★. Outside the solar orbit there is a large scatter of orbital velocities and measurements are scarce.

spiral galaxies seen face-on leads to the conclusion that while the inner parts of the discs show very regular spiral structure, the latter is heavily perturbed in the outer parts of discs.

Inspection of pictures of external spiral galaxies seen edge-on reveals well-distinguished, narrow, dust-gaseous thin discs extended up to the visible borders of these galaxies. Such a thin disc structure is apparently perpendicular to the galactic rotation axis. On the other hand, the stellar (especially evolved) component forms the thick disk in our Galaxy (and in other spiral galaxies), apparently influenced by other forces than just the gravity of the central bulge and the centrifugal force. Thus its kinematics is much more complex than that of the thin disc. This may be a result of a strong disturbing influence of possible merging effects. To properly identify these sources we first need a clear picture of the true, “basic” kinematics of the original thin disc, e.g. its rotation curve. We should expect to obtain this for our Galaxy from the observed motion of the most representative and reliable thin disc tracers. The latter are the interstellar clouds and OB stars recently formed out of this diffuse matter.

In this work, we introduce a new method for estimating the Galaxy rotation curve based on measurements of intensities and radial velocities of interstellar CaII lines in the optical wavelength range, with just a single assumption: circular orbital motion of interstellar, optically thin clouds.

The presence of DM inside and/or around our Galaxy was recently questioned by Moni Bidin et al. (2012). Estimating the dynamical surface mass density at the solar position between $Z = 1.5$ and 4 kpc from the Galactic plane, the authors concluded that the local density of DM is at least an order of magnitude below the standard expectations. However, Bovy & Tremaine (2012) used the model with different assumptions (although simplified) and concluded the accordance of observations with the standard DM paradigm. This fact makes it very important to carry out other observational tests of the existence of DM; that the same data interpreted using different models leads to contradictory conclusions proves that that observational data are insufficient.

Our recent papers (Megier et al. 2005, 2009) demonstrated two important facts. First: interstellar space in the thin disk of the Galaxy is rather evenly filled with optically thin clouds, revealed by the CaII H and K lines. The same Doppler components that reveal the presence of many clouds along a sightline can be found in NaI and KI strong interstellar lines. Second: the column density of CaII and, in practice, the equivalent widths (EWs) of these lines since saturation effects are low; (the latter are much stronger in NaI lines) can be used to infer distances to the observed stars. With growing distance from the Sun (in the outer part of the Galaxy) the observed Doppler components are more and more Doppler shifted along any sightline—probably due to the differential rotation of the Galaxy.

The direction towards $l = 135^\circ$ looks especially interesting. Trigonometry, as shown in Fig. 2, shows that the blue-shifts of Doppler components grow with distance in this direction. This is important because we have good observations of Doppler splitting, even with medium resolution, and because the broadening of the lines, caused by the Doppler splitting, prevents them from strong saturation. One should expect that the Doppler shifts grow with distance and thus the most

blue-shifted Doppler components (in the $l = 135^\circ$ direction) are formed in the most distant clouds (assuming that a sightline intersects a couple of clouds at different distances). It is interesting to check whether the same Doppler structure can be found in other interstellar features and whether the observed stars, which are the most distant objects along a sightline) share the radial velocity with the most distant clouds.

Figure 3 clearly shows that in any of the interstellar features one can see the same set of Doppler components. Apparently the Doppler shifts grow with distance, which makes possible distance estimates to individual clouds. One can observe two important facts: intensity ratios of the same radial velocity components of features, likely to originate in the same environments, are different; radial velocities of the observed stars may not be related to any interstellar component. The stars we are interested in are likely to be members of clusters or OB associations; many of them belong to binary systems. Thus, these stars are likely to orbit around local gravity centers, while interstellar clouds, situated far away from any such centers, only show orbital motion (around the Galaxy center) and, along the chosen sightlines, the radial components of orbital motion only are seen. Thus interstellar clouds are much better tracers of the radial velocity components of orbital motion than stars. In the $l = 135^\circ$ sightline, the farther a cloud is, the more (in general) it is blue-shifted.

The published rotation curve of our Galaxy has in many cases been based on radial velocities of CO radio lines (Clemens 1985). In these cases, distances were estimated to the observed stars. It seemed natural that molecular lines originated in relic clouds from which the OB stars recently formed. It seems quite natural that all interstellar molecules are spatially correlated. If the latter is true one can expect some intensity correlation between column densities of any two interstellar molecules (except, perhaps CH^+). We have compiled CO column densities from several publications in Table 4. We measured column densities of the easily accessible CH radical for these targets. Figure 4 demonstrates a reasonably tight correlation between the two species. This favors the hypothesis that the two molecules are spatially correlated. Thus their radial velocities can reasonably be expected to be identical.

Figure 3 clearly demonstrates that the main Doppler component of the CH 4300 Å line is of a different velocity to the SiIII stellar line shown (and, consequently, is formed in a cloud situated much closer to the Sun). However, the weaker CH components are still visible as far towards the violet as those of the CaII lines. These severely shifted components of CaII and CH are of the same radial velocity and thus they clearly can only be radial components of the orbital motion of the most distant cloud. On the other hand the stellar line contains some additional velocity, likely to be caused by motion around the center of a local cluster or association. It is also evident that the distance to the strongest CH component is much less than that to either the star or the most distant cloud. Apparently translucent interstellar clouds, moving only around the galactic center, are the best tracers of the structure of the thin disc and of the kinematics of the latter.

Translucent interstellar clouds are reasonably evenly distributed in interstellar space. Ionized

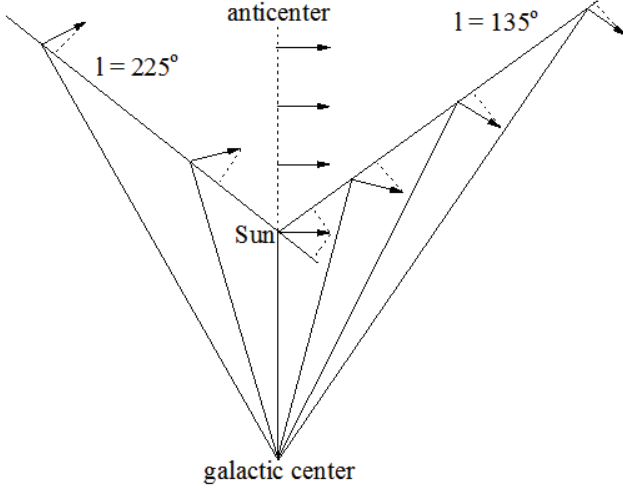


Fig. 2.— Schematic diagram showing that radial velocities towards the observer should increase with distance at $l = 225^\circ$ or decrease with distance at $l = 135^\circ$. Those observed towards the galactic anticenter should be close to zero if the rotation curve is flat and the orbits are circular. This diagram of the Galaxy is not made to scale; the aim is to explain the effects expected.

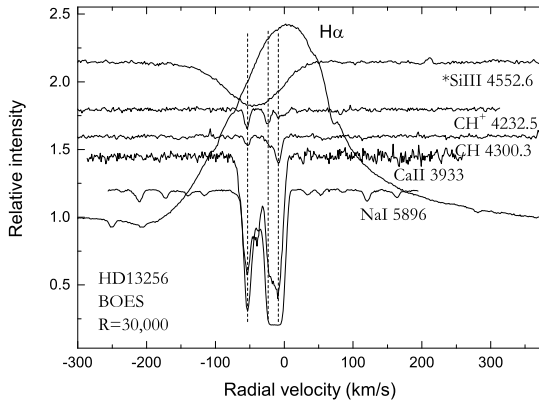


Fig. 3.— Radial velocity components seen in different interstellar features toward HD13256. It is important that the main CH component does not share the radial velocity of the stellar line. The strongest CH^+ component is apparently formed near the star, while the strongest components of neutrals are formed far away from the star but much closer to the Sun.

Table 4: Column densities of CH and CO interstellar molecules. YS – Sheffer et al. (2007), b – Burgh et al. (2007), S – Sonnentrucker et al. (2007), Lyu – Lyu et al. (1994). CH – our measurements.

Star	N(CH) $\times 10^{12}$	error	N(CO) $\times 10^{15}$	error
HD22951YS	21.36	1.56	0.18	0.01
HD23180YS	12.54	1.24	0.68	0.01
HD24398YS	23.52	2.91	1.79	0.05
HD24534b	22.3	2.61	13.49	6.5
HD27778b	38.05	3.22	11.22	3.8
HD73882S	34.02	1.7	35.5	17
HD91824b	6.75	1.35	0.04	—
HD99872YS	13.35	0.03	0.45	0.04
HD147888S	21.84	0.04	2	0.38
HD149757Lyu	25.66	0.82	1.58	—
HD154368YS	60.54	1.07	2.67	0.55
HD163758b	7.62	0.35	0.03	—
HD203374YS	23.34	0.28	2.55	0.43
HD206267b	26.4	4.71	12.9	4.5
HD207198b	45.21	5.62	3.4	1.7
HD207538YS	44.34	4.07	2.34	0.24
HD210121S	30	2.73	6.76	1.25
HD210839b	33.43	1.86	2.6	0.5
HD303308b	10.64	0.65	0.04	—

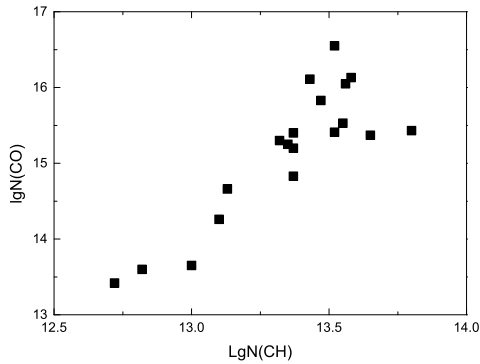


Fig. 4.— Correlation between column densities of CO and CH molecules for the stars in Table 4. A positive correlation is obvious.

Ca clouds seem to be good representatives of the gaseous thin galactic disc, supposedly better than any other of its constituents: NaI lines are usually completely saturated, making them useless, KI lines are in many cases too weak to allow all the components to be traced; the same latter problem also occurs for molecular features. Objects which appear to be unevenly distributed are interstellar clouds, revealed by molecular lines (Fig. 6). As seen from Fig. 3, molecular lines are very likely to be formed in all translucent clouds, but many components are very weak and thus fall below the detection limit. It is commonly accepted that OB stars are spatially related to molecular clouds out of which they have recently been formed; however, such remnant clouds are not necessarily situated along our sightlines. If an interstellar cloud shares the radial velocity with the star it may be such a relic object. If the radial velocity is drastically different, then the cloud is likely to be far away from the observed star; see Fig. 3. Thus, it is very risky to use distances calculated for OB stars and radial velocities of the main (strongest) components of molecular lines. Apparently the CaII features originate in many individual clouds, thin enough to get very strong lines that are not heavily saturated (Fig. 5). On the other hand, the main components of CH or CN spectral bands may be strong in the spectra of nearby objects and very weak in distant ones (Fig. 6, Fig. 3).

The observed scatter in the published rotation curves may indicate not only significant errors in the distance (and uncertainties in the radial velocity) determinations of the tracers used, but also more complex intrinsic kinematics of the outer disc. Moreover, in all the above mentioned rotation curve determinations, little attention has been paid to the question of the representativeness of the (most distant) used tracers of the galactic disc. The most distant tracers, used to do measurements depicted in Fig. 1, may be non-members of the Galaxy. Their rotational velocities are very large and the distances are equal to that of the LMC. We expect that thin disc objects, OB stars and gas clouds, to be the most reliable members of the thin galactic disk. The tiny clouds revealed by the H and K lines fill the disc almost continuously (Fig. 5) and thus all of them dynamically belong to the Galaxy beyond any doubt because the radial velocities grow continuously up to the observed star – apparently formed recently inside the thin galactic disc.

The main purpose of the present paper is to delineate and analyze the rotation curve of the outer part of the gaseous disk of the Galaxy, over the distance of a few (up to 3–4) kiloparsecs beyond the solar circle, where the flat or Keplerian character of the rotation curve should be clearly distinguishable. As stated above, this part of the published galactic rotation curves suffers large uncertainties because of insufficient statistics of the tracers observed, and because of large scatter seen in the individual measurements of distances and radial velocities. On the other hand, all the published Galactic rotation curves show a distinct dip in this region and the spatial localization of this dip is about 1–2 kpc beyond the radius where the observed density of the visible disk starts to decline (drop) outwards, which may suggest that these indicate the border of the Galactic Disk.

To construct the rotation curve over the selected regions we propose to use interstellar gas clouds revealed by CaII spectral lines. This choice is based on at least two reasons:

- recently we have demonstrated (Megier et al. 2005, 2009) that the equivalent widths of

interstellar CaII lines, observed in the thin Galactic disk, correlate tightly with distance.

- the relatively low level of saturation of even very strong CaII (in the sense of equivalent width) lines, seen in the near UV, clearly proves that the whole space in the Galactic disc is quite evenly filled with rather tiny (optically thin) clouds, producing (almost) unsaturated components, more and more Doppler shifted along a chosen sightline—probably due to the differential rotation of the Galaxy (see Fig. 5).

These two reasons make CaII clouds the best tracers of the thin disk structure.

Let us assume that the equivalent widths of the near UV CaII lines increase with distance by adding subsequent optically thin clouds—thin enough to produce unsaturated H and K lines. In general these clouds participate in the differential rotation of the Galaxy. Depending on a chosen direction, if they move on circular orbits, radial velocities of more and more distant clouds should be more and more blue- or red-shifted (Fig. 5, Fig. 2). Thus the most shifted H and K Doppler components (which share radial velocities with all other interstellar absorptions but are stronger and thus best seen) should measure the radial velocity of the most distant cloud which should be very close to that of the observed star: the farthest object along the sightline (Fig. 8). The total column density should measure the distance to the observed star, or more precisely, the farthest CaII cloud along the line of sight (Fig. 3). The formula derived by Megier et al. (2009) from 262 sightlines is:

$$D_{CaII}[\text{pc}] = 77 + \left(2.78 + \frac{2.60}{\frac{\text{EW(K)}}{\text{EW(H)}} - 0.932} \right) \text{EW(H)}, \quad (1)$$

where EW(H) is measured in mÅ. This formula can be applied if EW(K)/EW(H) > 1.32, which guarantees that the saturation level is low enough. Each pair of measurements: distance (from CaII column density) and radial velocity (from CaII line profiles) can be done from the same spectrum. This strongly reduces the number of observations needed to construct the rotation curve and removes the ambiguity that follows from unknown velocity components in stellar spectra. Let’s emphasize that stellar lines observed in spectra of hot, OB stars are broad which makes difficult to resolve individual Doppler components. On the other hand our method allows the selection of well-defined Doppler components of CaII lines to measure the radial velocity of the most distant clouds along the chosen sightlines. Apparently, the main components of other interstellar lines, in particular, molecular ones, are likely to originate in clouds situated much closer than the observed OB stars—see Fig. 5 and Fig. 3.

As it was shown by Megier et al. (2009, see their Fig. 6), the CaII-method exhibits a good agreement with distances of OB-associations, i.e. Eq. 1 should give reasonable distance estimates up to ~3 kpc in the Galactic plane. In the current study we slightly exceed this value, though most of our targets are closer than 3 kpc. The good agreement of CaII distances and those based

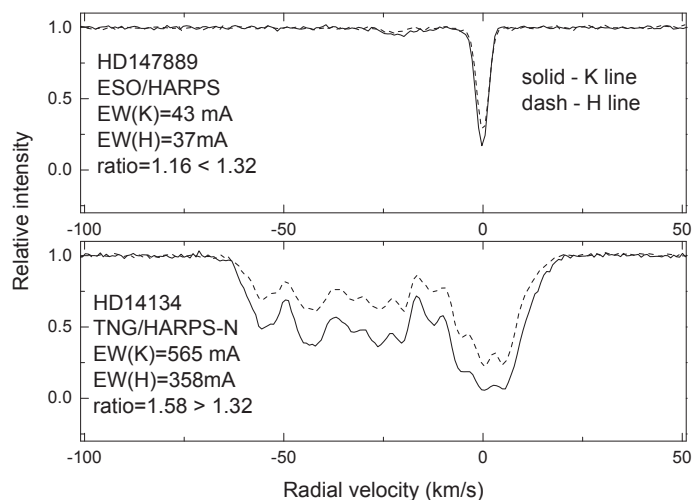


Fig. 5.— Evidence that the clouds revealed by CaII lines observed towards the direction $l = 135^\circ$ evenly fill the galactic disk (number of components grows with distance, each new one is more and more blue shifted) and thus, that the H and K lines remain free of strong saturation while saturation may be evident towards nearby objects.

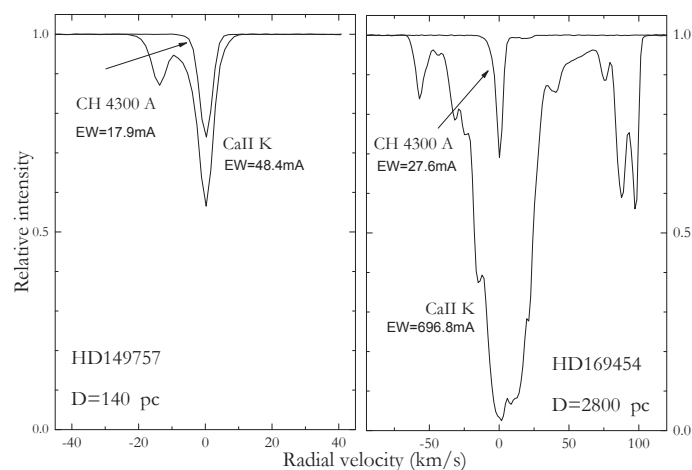


Fig. 6.— Example of how distances grow with CaII line intensity. The CH radical is apparently abundant only in relatively few clouds along the long sightline, making it a poor tracer of galactic rotation.

on OB-associations (Megier et al. 2009, see their Fig. 6) is not the only proof of the correctness of CaII distances. Fig. 5 proves that the CaII clouds are distributed quite evenly, at least in the $l=135$ direction. The distance to HD 14134 is 2.2 Kpc according to both CaII and spectroscopic parallax methods.

How valid is our assumption that our CaII absorbers rotate on circular orbits? Circular orbits are usually assumed, but our method allows this assumption to be checked observationally. The stars observed towards the galactic anticentre are listed in Table 3. Figure 7 shows the profiles and radial velocities of the CaII K line, seen in the spectra of our targets. The assumption of circular orbits is clearly a good approximation for this choice of tracers.

Neither binarity of the chosen targets (clouds) nor pulsations affect the observed radial CaII velocities (Fig. 10). Also, uncertainty of determination of the profile center is much lower in the case of interstellar absorption lines than for the stellar spectra of fast rotators. With a resolution of $R > 30,000$, the former is better than ~ 1.3 km/s. The distance estimates only require one calibration: distance vs. intensities of CaII lines—rather than requiring several calibrators, as is the case for spectroscopic parallax. This provides another argument in favor of using the gaseous component of the thin disk to determine the rotation curve of the Galaxy. This has not been done previously, although, quite recently, Bobylev & Bajkova (2011) used the CaII distances from our work by Megier et al. (2009) to determine kinematical properties of the local part of the Galactic disc. We stress the point that among interstellar features seen in stellar spectra, only interstellar CaII lines show a reasonable choice of Doppler components, correlating well with distance, in contrast to other interstellar atoms/molecules. CH lines and other similar features may trace the dust lanes in spiral arms, one of which is quite close to the Sun—about 1 kpc. Since the CaII clouds are ubiquitous, filling the galactic disc almost uniformly, they form the dominating gaseous thin disc component of the Galaxy (Fig. 5).

The selection of a proper tracer to establish the Galactic rotation curve is crucial. Until now radial velocities have been measured either for H_α lines of HII regions or for molecular features. Distances are usually those of the observed OB stars, sometimes determined by the ZAMS fit. Figure 3 demonstrates the ambiguity of the choice made. It is natural that the radial velocity of H_α is very different from that of any component of the CH molecule.

Moreover, the radial velocity of the stellar SiIII 4553 Å line is close to one of the components of CH. We can choose the most blue-shifted component of any of the interstellar lines as the farthest one. The even distribution of CaII clouds makes the choice most natural. Thus only the tiny clouds revealed by the CaII lines allow to reasonably relate distances and radial velocities; the latter measured with a very high precision of the order of 1 km/s. The kinematics (rotation) of this component seem to contain a key for checking for the possible presence of local DM in the Milky Way. The simplest way to find support for the existence of local DM is to compare the observed rotation curve, based on CaII tracers, with e.g. the “Keplerian” curve determined by the distribution of the visible matter only and the “flat” curve. In opposite to many “model” recent

works (e.g. Bovy et al. (2012), Xue et al. (2008)) our attempt may belong to the “clean” category in the sense it is based on direct measurements of individual objects; instead of being an attempt to fit a model which follows a set of assumptions. This is why we do not construct any model, but just assume either Keplerian or flat rotation curve.

To construct a kinematical map of the outer part of the Galaxy one needs reliable Galactic disc tracers with well-determined distances and radial velocities. Uncertainty in determining the rotation curve in the outer part of the Galaxy follows the uncertainties of estimates both of these.

In the case of HI clouds, the distances are inferred from their angular sizes; this requires assumptions about their linear sizes (which are very uncertain). The HII regions should be at the same distances as those of their central OB stars. However, the distances to OB stars, based on spectroscopic parallax, are uncertain for several reasons:

- calibrations of absolute magnitudes for a given spectral type and luminosity (Sp/L) are uncertain because of poor statistics of OB stars that have reliably measured trigonometric parallaxes
- all stellar parameters (in particular m and M) should be used at the same phase of possible variability; calibrations of M for different variability phases do not exist
- calibrations of intrinsic $B - V$ colors for a given Sp/L (the latter frequently seriously flawed); these are less important but non-negligible
- determinations of extinction curves and total-to-selective extinction ratios which may vary from object to object; using a mean extinction law may lead to very serious errors—on average growing with distance but not possible to be properly estimated
- the unsolved problem of neutral (grey) extinction.

To illustrate this, let us consider two stars from our list (Table 2): BD +59-456 and BD +60-493. According to the Simbad database their Sp/L’s are B0.5V and B0.5Ia, respectively. For distant objects, which are needed for determining the rotation curve, we cannot expect many independent classifications in the literature. Using the spectroscopic parallax method we estimated the distances to the above objects as 1600 and 2800 pc respectively (assuming $R_V=3.1$). Fig. 9 demonstrates our high resolution spectra of both targets. It is evident that the spectral type is the same (note the identical ratio of HeI/HeII lines) but the luminosity classes stated in Simbad are evidently incorrect. Indeed, the spectral lines in the “dwarf” are narrower than in the “supergiant”. If BD+60-493 has been classified correctly, then BD+59-456 should be of the luminosity class Ia-0 rather than V and thus, according to Schmidt–Kaler (1982), be of the absolute magnitude $M=-8.2$. This would double the spectroscopic distance. In the Schmidt–Kaler (SK) system, there is no intermediate Sp/L allowing for an interpolation between an absolute magnitude of -6.9 (for Ia) and or -8.2 (for Ia-0). If our method, based on CaII lines, is applied, the distances are 3300 and 3000 pc, respectively, which is very reasonable.

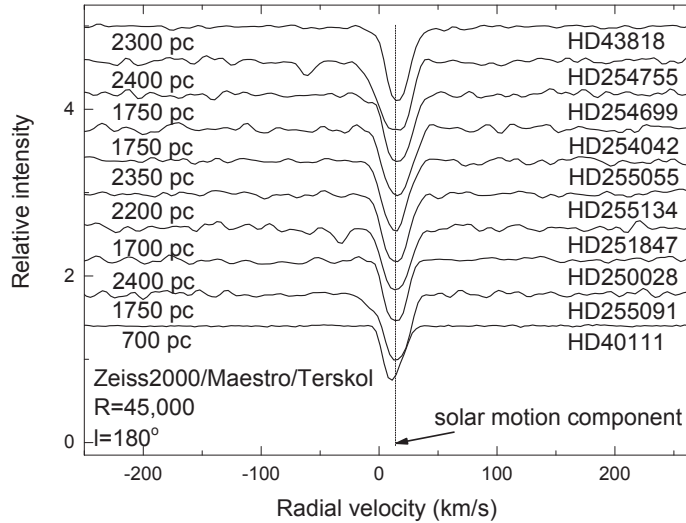


Fig. 7.— CaII lines observed towards the galactic anticentre. There is no obvious Doppler splitting. The dashed vertical line represents the solar motion radial component relative to the LSR. The orbits of presented CaII clouds seems are circular!

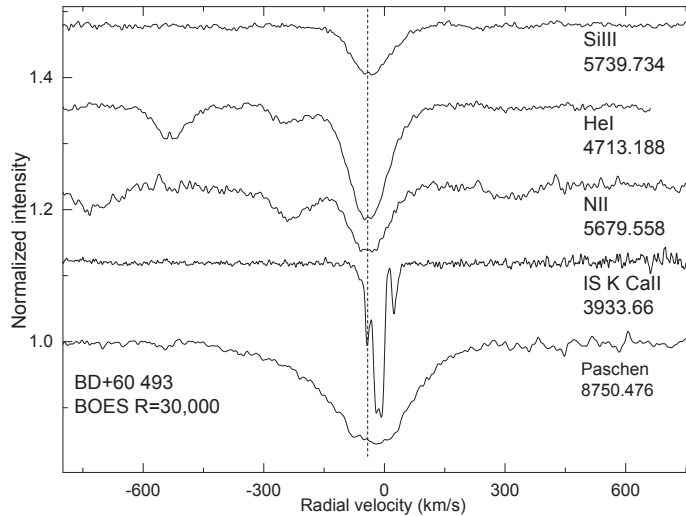


Fig. 8.— Radial velocities of interstellar clouds growing up to the limit of the stellar radial velocity in the direction to $l = 135^\circ$. The interstellar clouds are situated between the observer and the star, i.e. the star is, among the depicted objects, the most distant one and so its radial velocity (negative) should be the greatest in that direction along this sightline.

In practice, all these uncertainties add one to another and the final result (distance) appears to be very questionable. It is not possible to reliably estimate errors in distance estimates made using spectroscopic parallax. Our method only involves the total intensities of CaII lines (distance—Fig. 6) and the positions of the most blue-shifted Doppler components (radial velocity—Fig. 3, Fig. 8). These do not need any calibration except for the observed relation of CaII column density and parallax (Megier et al. 2009). Our measurements are reasonably precise until the CaII lines become heavily saturated ($EW(K)/EW(H) > 1.32$). Moreover, any distance–radial-velocity pair can be reliably determined from a single spectrum. Stellar binarity, variability and possible motions around local gravity centers (e.g. clusters) do not influence either distance or radial velocity measurements (Fig. 10). The rotation curve may be constructed from a homogeneously measured set of distances and radial velocities for interstellar CaII clouds, which fill the galactic disc much more evenly than stars and clusters, being for the same reason the dominant gas component of the thin Galactic Disc.

Here, we propose a new tracer of the Milky Way rotation curve: CaII clouds, possessing a variety of advantages in comparison to “classic” tracers, mainly because of requiring fewer assumptions, thus reducing sources of systematic error.

3. Method

Assuming circular orbits of objects (stars and clouds) in the galactic disc we have selected two directions (galactic longitudes 180° and 135°) which enable checking galactic rotation according to Fig. 2. In Fig. 2 it is shown how the observed radial velocity should decrease with increasing distance from the Sun in the 135° direction. In the direction to the Galactic anticentre the observed radial velocity, related to the local standard of rest (LSR), of every object is expected to be close to zero (if it is true that the orbits of thin disc objects are circular).

The Sun does not move on an exactly circular orbit. The total velocity of our star, relative to the LSR, defined by young O–B5 stars and B8–A0 supergiants in the distance range 0.2–3.0 kpc, derived using the Skymap Catalogue (Zhu, 2006) distance scale, is $V_s = 20.1 \pm 0.4$ km/s towards $l_\odot = 51^\circ.2 \pm 1^\circ.2$ and $b_\odot = +22^\circ.9 \pm 1^\circ.1$. Using the Hipparcos distance scale the above values are respectively: $V_s = 16.9 \pm 0.4$ km/s, $l_\odot = 47^\circ.2 \pm 1^\circ.3$ and $b_\odot = +22^\circ.9 \pm 1^\circ.2$ (Zhu 2006). Miyamoto & Zhu (1998) previously determined somewhat different values: $V_s = 19.1 \pm 0.5$ km/s, $l_\odot = 49^\circ.2 \pm 1^\circ.6$ and $b_\odot = +21^\circ.9 \pm 1^\circ.3$. In this paper we have adopted the average values $V_s = 18.5$ km/s, $l_\odot = 49^\circ.2$ and $b_\odot = +22^\circ.9$; our model rotation curves are calculated using the latter averages. The solar motion with respect to the LSR is especially useful for our method, since it is nearly perpendicular to the direction $l = 135^\circ$, i.e. it has a very weak influence on our measured radial velocities. This is why the radial velocity is close to zero for nearby objects at $l = 135^\circ$ (see Fig. 11).

On the other hand our estimated value of the Sun’s radial motion, derived from radial velocities of CaII clouds in the direction $l=180$ is close to 12km/s (Fig. 7) quite accordant to that, given by

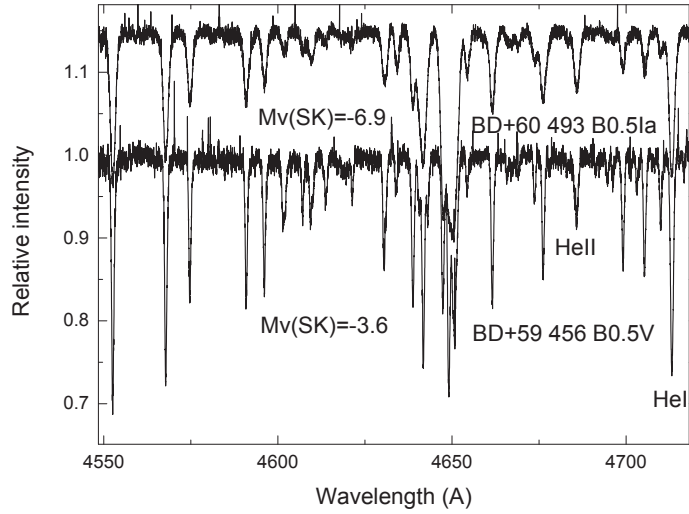


Fig. 9.— Spectral classification errors leading to huge errors in distances based on the spectroscopic parallax method.

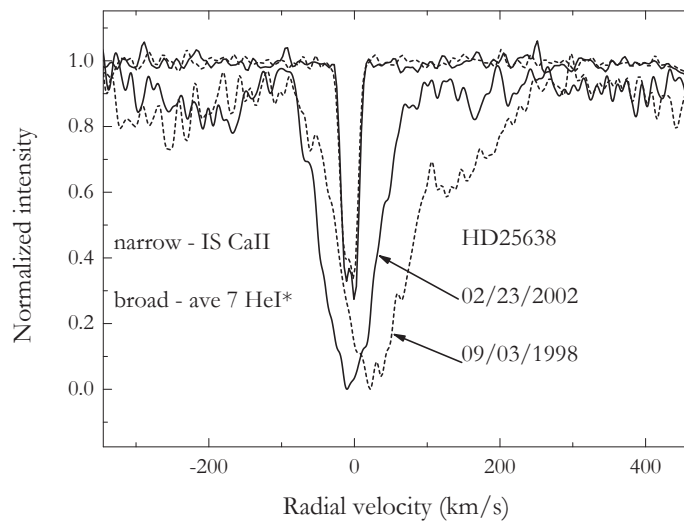


Fig. 10.— Illustration of how binarity or pulsations of the stellar object can influence the measured radial velocity. The radial velocity measured using CaII lines remains unchanged.

Bovy et al. (2012).

Our proposed construction of the galactic rotation curve is based on distance estimates and radial velocities of the most blue-shifted Doppler components of the ionized calcium (CaII) lines in the direction $l = 135^\circ$. In the direction of the anticentre, the expected radial velocities are zero: in the current study we check this as a control on the validity of our method.

The rotation curve is a smoothed average of the velocity field; it is the relation that gives the velocity of rotation on circular orbits with respect to the center of a galaxy as a function of distance from its center. However, various deviations from circular movement, e.g. peculiar movements of stars and clouds, expansion, streaming in spiral arms have to be included in consideration as well. The velocities of stars and gas are determined (mainly) by the gravitational potential, generated by the galactic mass distribution. The rotation curve in the galactic plane is usually determined almost exclusively from radial velocities (due to very uncertain data on proper motions) of chosen (distant) tracers with the assumption they do move on circular orbits around the galactic center. The latter assumption finds strong, observational support in our case (Fig. 7). Until now, circular motion has been assumed without evidence because no other assumption was sufficient for modeling galactic rotation. Our observational evidence is an independent test showing that the assumption seems well grounded in empirical data for our choice of tracer.

We adopt the assumption of circular orbits in the galactic gaseous disc (see Fig. 2); the radial velocities V_{rad} towards the observer of objects situated near the Galactic plane can be transformed into the circular rotation velocity by inverting the following relation (derivable with the sine rule),

$$V_{\text{rad}} = (\omega_{\odot} - \omega)R_{\odot} \sin l \cos b, \quad (2)$$

where ω_{\odot} is the angular velocity at the Sun position, i.e. (V_{\odot}/R_{\odot}) , ω is the angular velocity at the position of the considered object (V_{rot}/R_*) , R_{\odot} is the galactocentric distance of the Sun, V_{\odot} and V_{rot} are the rotation linear velocities of the Sun and the considered star while l and b are the galactic longitude and latitude of the object respectively. The galactocentric distance of the object R_* is determined from the cosine formula

$$R_* = \sqrt{R_{\odot}^2 + (d \cos b)^2 - 2R_{\odot}d \cos b \cos l} \quad (3)$$

where d is the distance of the object from the Sun. The distance d can be estimated from the column density of CaII for the translucent clouds (from H and K lines seen in spectra of young stars). Both the above formulae allow the construction the rotation curve in two forms: ω vs. R_* and V_{rot} vs. R_* . In our approach, instead of the ω vs R_* or V_{rot} vs. R_* , we will check the shape of the rotation curve directly on the observed V_{rad} vs. d plane. This allows to use of almost “raw” measurements; to obtain the parameters shown in Fig. 1, one must convert the radial velocities to orbital ones using the above formulae and assuming certain values for R_{\odot} and V_{\odot} —both of them known to an accuracy of no better than 25%.

The most promising approach after assuming circular rotation seems to be to test the rotation curve in the sector of the Galactic disk around $l = 135^\circ$, available to observations from the Northern

hemisphere. We have collected a big sample of high resolution spectra inside this sector (50 OB stars), some of them very distant. A very simple model, assuming R_{\odot} and V_{\odot} as stated above (Sofue et al., 2009), allows evaluation of the relation between the distances along this sightline and the expected radial velocities. We need to penetrate the galactic disk sufficiently deeply with our “milestones”.

Assuming $R_{\odot} = 8.0$ kpc and $V_{\odot} = 210$ km/s, we used the above equations to draw the relations of V_r vs. d for the “flat” and “Keplerian” rotational curves for this selected galactic longitude.

4. Observations

As stated above, we selected the directions with galactic longitudes 135° and 180° for observations; the objects used for our test are close to the galactic equator, being situated not farther than 100pc from the galactic plane.

Spectra of the selected objects have been obtained during several runs spanning the period 1999–2014, using the Bohyunsan BOES (b) and Terskol MAESTRO (t) echelle spectrographs. The BOES echelle spectrograph (Kim et al., 2007) is attached to the 1.8m telescope of the Bohyunsan Observatory in Korea. The spectrograph has three observational modes providing resolving powers of 30,000, 45,000 and 90,000. The lowest resolution, enabling observation of quite faint, heavily reddened, distant objects was used in most cases. In any mode, the spectrograph allows the whole spectral range from ~ 3500 to $\sim 10,000$ Å, divided into 75–76 spectral orders, to be recorded. The selected stars are listed in Tables 2 and 3 together with their galactic coordinates, distances, and orbital and heliocentric radial velocities.

MAESTRO (MAtrix Echelle SpecTROgraph) is a three branch cross-dispersed echelle spectrograph installed at the coude focus (F/36) of the telescope ZEISS-2000 at the Terskol Observatory (Caucasus mountains). It was designed for stellar spectroscopy with resolutions from 45,000 to 190,000 in the spectral range 3,500–10,000 Å. Using the lowest resolution mode (sufficient for our programme) one can reach spectra of objects as faint as $\sim 10^m$ with a signal-to-noise (S/N) ratio not less than 70, sufficient for measurements of CaII line.

Two spectra, depicted in Fig. 5 are high resolution spectra, acquired using the HARPS spectrograph at the 3.6 m ESO telescope (HD147889) and HARPS-N at the 3.5 m Telescopio Nazionale Galileo. These were used here only in the justification of our method, and not for the measurements presented in this work.

All the spectra were reduced and measured in a standard way using the packages IRAF (Tody 1993) and DECH³.

³<http://gazinur.com/DECH-software.html>

5. Results

We have measured, for all available targets, both distances and radial velocities using the CaII H and K lines (Tables 2 and 3). In every case we used the radial velocity of the most blue-shifted Doppler component (Fig. 8) to construct the galactic rotation curve. The precision of the radial velocity is in every case no worse than 1.3 km/s (for the spectra with $R=30,000$). The accuracy of distances is likely to be worse; however, because these are based on a single calibration, they are much more reliable than those obtained using spectroscopic parallax. The latter suffers because of systematic uncertainties related to determination of spectral type (as shown above—Fig. 9), variability of brightness (usually unknown in the case of distant, rarely observed objects) and the reddening index (R_V) of the object studied.

To compare the rotational curve determined in the way described above for the thin Galactic Disk with the kinematical properties of other possible tracers of this structure, we restricted the choice of “other” tracers to open clusters, which are massive and thus less susceptible to random gravitational disturbances. Moreover, open clusters are too young to be incomers from recent mergers. Our present analysis is thus restricted to the objects situated in very close to the galactic equator and formed/born in the places they are observed in.

For the same reason we do not intend to interpret the observed (published) rotational curves of other galaxies as these curves obviously present kinematics composed from a mix of many kinds of tracers: those representing the thin disk as well as those significantly gravitationally disturbed, which create substantial scatter in the average rotational curve of our Galaxy (Fig. 1 of Sofue et al., 2009). Our observations and analyzes are restricted to the thin disc of our Galaxy. This is also why we do not relate our results to galactic rotation curves inferred from evolved, giant stars like those of Xue et al. (2008) or Bovy et al. (2012) as these results concern other galactic population with larger velocity dispersion, while our considerations concern exclusively thin disc, young objects.

The results of our measurements are collected in Tables 2 and 3. Our observed targets are shown as filled circles in Fig. 11. In this figure, two model rotation curves for the Galaxy, i.e. flat and Keplerian, are also shown. The reasonably large scatter seen in Fig. 11 most likely is an effect of the resolution—not high enough to resolve all Doppler components. Both the resolution and S/N ratio limit the accuracy of distance estimates, which are the main source of the rotation curve uncertainties. In Fig.11 we also show (as open diamonds) seven open clusters (data from the literature, see Table 1) seen at $l = 135^\circ$. We have selected only the clusters whose radial velocities were determined using at least 4 objects; for the vast majority of known clusters, radial velocities are based on 1–3 stars. The positions of distant clusters clearly agree with those of our CaII clouds within the observed scatter.

However, the distances to open clusters are uncertain in many cases. According to the compilation by Subramanian & Bhutt (2007) the published distances to e.g. NGC 7245 vary between 1925 and 2800 pc, while those to IC166 cover the range from 3300 to 4800 pc. These high uncertainties must be reflected in the rotation curve. The above mentioned clusters have not been used

in our analysis. Once again, our method of determining distances using CaII interstellar lines is more accurate and leads to more homogeneous results.

Our measurements of radial velocities have, however, uncertainties related to the relatively low resolution of our spectra. Our first estimate of the radial velocity of HD2905 (from our spectra) was -15 km/s. We have also checked ultra high resolution results published by Welty, Hobbs & Morton (2003). The authors clearly demonstrate the Doppler component at -27 km/s. The latter value was finally adopted in our work. An example that the higher resolving power reveals more blue component in the direction $l = 135^\circ$ is shown in Fig. 12. An increase in resolution might influence our results shown in Fig. 11 and Fig. 14. Several very narrow Doppler components might be found instead of a seemingly single one at lower resolution. This effect would cause our estimates, the filled circles in Fig. 11 and Fig. 14, to be shifted downwards in the diagrams. Such shifts would make our conclusions even stronger, as they would move points farther below the flat curve than they presently lie.

In the $l = 180^\circ$ direction (Fig. 7), the our data is scarce but the scatter of radial velocities is very small. Apparently *all* of the observed radial velocities are almost exactly equal to the solar motion component with respect to the LSR (almost identical to that of Bovy et al. (2012)), providing strong evidence that CaII clouds are orbiting around the galactic center on circular orbits. In addition, among our targets, there appears to be no systematic trend of radial velocities as a function of height from the galactic plane (Fig. 13). Apparently our samples represent only the thin galactic disc.

Equations (2) and (3) enable the conversion of our distance and radial velocity measurements to the plane: distance from the galactic center versus orbital speed, i.e. we plot the rotation curve using the same parameters as in Fig. 1. We reproduce the set of Sofue et al. average points and show our converted measurements. As demonstrated in Fig. 14, our points are scattered around the Keplerian rotation curve as in Fig. 11. However, to make the latter plot, we had to assume certain values for the orbital radius and the speed of the Sun. These are assumed to be the same as those of Sofue. However, the orbital radius of the Sun available in the literature ranges between 7.5 and 10 kpc and the Sun’s orbital velocity is reported between 200 and 250 km/s (Brand & Blitz (1993)).

We checked the agreement of the postulated rotation curves, based on different solar orbital velocity and its distance from the center of the Milky Way with the observed points; the latter clearly follow the “Keplerian” curve. Let’s emphasize that the Sun’s specific velocity is almost perpendicular to the $l=135$ direction and thus its Doppler component along this sightline is practically zero.

The positions of points in Fig. 14 depend on the assumed values of solar radius and orbital velocity; on the other hand in Fig. 11 only the theoretical curves depend on these values, while the points, representing original measurements, do not. Thus, we consider the plot in Fig. 11 more reliable. Such a plot may be used to select the most likely correct values of the orbital parameters

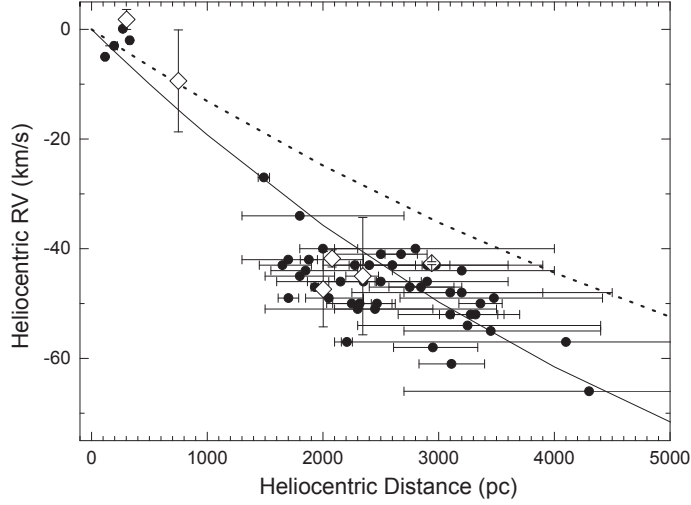


Fig. 11.— Radial velocity curve for the direction $l = 135^\circ$. “Flat” rotation (dotted line) and Keplerian (solid line) theoretical curves are shown. Filled circles represent our observed objects (CaII clouds) and open diamonds represent literature data for open clusters.

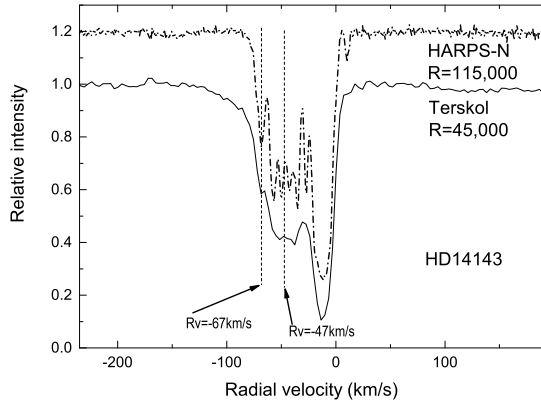


Fig. 12.— Higher resolving power applied to a target in direction $l = 135^\circ$ reveals more blue component, i.e. leads to increasing the discrepancy the observed data with the “flat” model (see Fig. 11).

of the Sun (radius of the orbit and velocity).

6. Discussion

Let us check whether our result agrees with other measurements, in particular, with the rotation curve based on spectroscopic parallax distances. Table 5 contains our targets with the following data: Sp/L (taken from Simbad together with photometric data), radial velocity of the star, radial velocity of the CH main features, spectrophotometric distance from the Sun and the same distance converted to a galacto-centric distance. As shown in Fig. 3, the main component of the CH line is usually closer than the observed star. The galactic rotation curve was in several cases built using CO lines’ velocities and stellar distances. We have collected the published CO column abundances and related them to our own measurements of CH abundances (Table 4). Both abundances are correlated in Fig. 4. It is evident that the abundances of the two species are correlated and thus it is reasonable to infer that they are also spatially correlated and that the radial velocities of the two species should be identical.

However, as shown in Fig. 3, the main component of CH originates closer to the Sun than to the observed star. Thus, using spectroscopic distances and CH radial velocities must lead to an incorrect result. The radial velocities of the main CH components are much lower than those of the most blue-shifted ones. This moves points in Fig. 11 up and mimics a flat rotation curve. In fact, the radial velocities should be measured for the most blue-shifted components which, in the case of molecular features, are barely visible in most cases (one can observe them only in very high S/N spectra).

It is also interesting how far our distance estimates coincide with the spectroscopic ones. Using the data from Tables 2 and 5, we have correlated our distances (from CaII lines) with the spectroscopic ones (Fig. 15). There is a correlation but there are several serious outliers.

The published classification of BD+59-456 is evidently flawed. Let us consider another object, HD13256, for which we have a high quality spectrum. The object is classified as B1Ia. We compare its spectrum with that of the B1Ia standard—HD148688 (according to Walborn & Fitzpatrick (1990)). Figure 16 demonstrates that HD13256 is probably of a later spectral type (since it lacks the HeII line that is clearly seen in HD148688) and of higher luminosity (the HI line is narrower than in HD148688). Thus, the star may belong to the luminosity class Ia-0, leading to a much higher spectroscopic distance, which agrees with that based on CaII lines.

Generally the highest luminosity OB stars are very scarce and thus it is very difficult to find two identical spectra which may lead to identical luminosities. Apparently all the outliers in Fig. 15 can be “corrected” to our CaII estimates by means of changing Sp/L’s within the commonly accepted errors. The published Sp/L’s are seriously flawed in many cases and thus it is practically impossible to apply these values if there is no possibility to check them using spectra of sufficient quality.

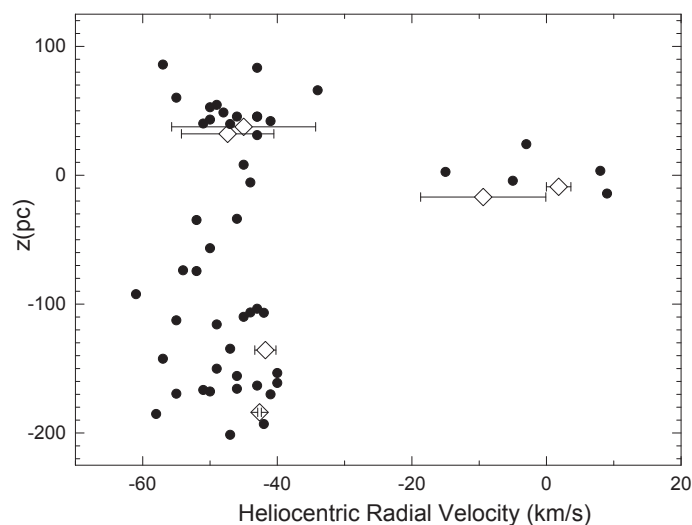


Fig. 13.— Distribution of radial velocities of our targets in the $l = 135^\circ$ direction. No systematic effect related to distance from the galactic plane is observed.

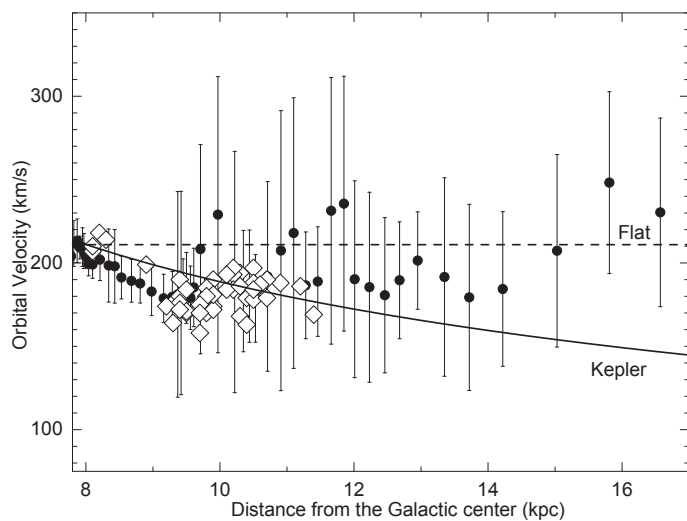


Fig. 14.— Comparison of our measurements (hollow diamonds) with the rotation curve of our Galaxy compiled by Sofue et al (2009). Our points fill the very important gap at 9 kpc from the Galactic center. Our measurements are obviously scattered around the Keplerian rotation curve. No distant points agree with the flat one.

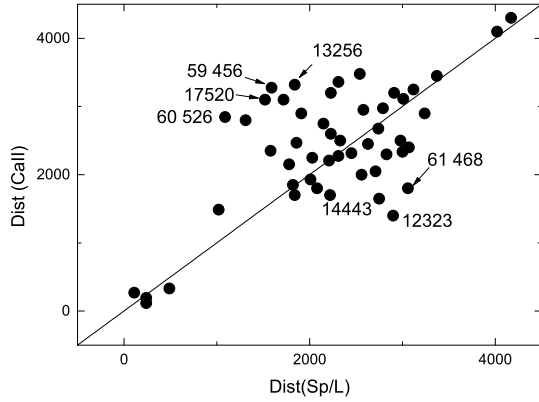


Fig. 15.— Comparison of our CaII distances with those from spectroscopic parallax. Some outliers (see Sect. 6) are marked in the plot.

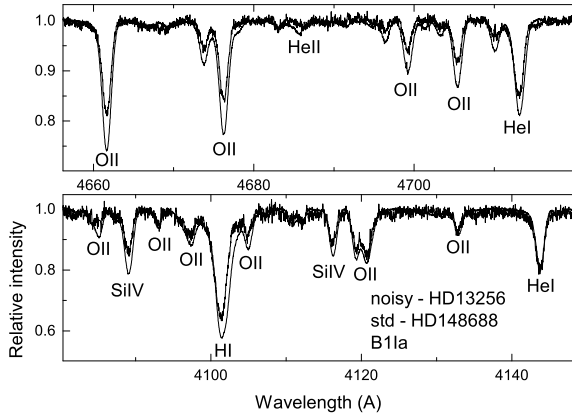


Fig. 16.— Comparison of the spectra of HD13256 (outlier) and HD148688 (B1Ia standard). HD13256 is likely to be a bit colder (no HeII line) and of higher luminosity (HII narrower).

Nevertheless, we check the rotation curve inferred from measurements of stellar distances (using spectroscopic parallax) and of radial velocities based either on stellar lines or interstellar molecular features—in our case the CH radical, well correlated with CO, as shown in Fig. 4.

The result is shown in Fig. 17. We have plotted two sets of radial velocities versus spectroscopic parallax distances. Dots represent radial velocity measurements based on stellar lines. The result is as expected: the scatter is much higher than that in Fig. 11. It follows from the phenomena discussed above: stars are members of multiple systems or of clusters and thus their radial velocities are sums of the orbital (around the galactic center) and local components. In spite of this, the stellar line radial velocities do favor the Keplerian rotation curve over the flat one, but less clearly than in Fig. 11. This demonstrates once again that measurements of interstellar CaII lines lead to much more precise values.

One can express a doubt whether the CaII distances are not systematically incorrect due to the declining gas density outwards the Milky Way disc. However, this should result in a systematically growing difference between the CaII distances and those following the spectroscopic parallax. This is apparently not the case (Fig. 15). Also, while using stellar spectroscopic parallaxes we get the same (Keplerian) rotation curve as while using the CaII method (Fig. 18, Table 5).

The squares in Fig. 17 represent stellar (spectroscopic) distances and radial velocities of the main components of the interstellar CH 4300.3 Å line. As shown in Fig. 3 the main CH components are usually formed in interstellar clouds situated much closer than the observed stars. Connecting their radial velocities with stellar distances is clearly improper. The radial velocities of CH should represent the most blue-shifted components of the CH lines; however, the latter are detectable only in very high quality spectra—in the majority of cases they fall below the detection level. The location of the squares shows why in some cases the rotation curve is reported to have rotation velocity growing outwards.

We have averaged our rotation velocities plotted in Figs 17 and 11 within in 500 pc bins, and show these in Fig. 18.

Now it is evident that the rotation curve built using traditional spectroscopic parallax to measure distances to OB stars and stellar lines to determine radial velocities is consistent with that based on CaII lines (apart from the outermost stellar point, which is based on only two objects). The only obvious difference is the scatter, being much greater in the case of using Sp/L distances and stellar line velocities, because of the reasons explained above. The method based on CaII lines is the more precise one.

The results of our distance and radial velocity measurements from CaII lines, being more precise than any others and thus best representing the kinematics of the Galaxy thin gaseous disk, clearly argue in favor of Keplerian rotation of the latter. We do not comment on the behavior of other galaxies than the Milky Way because our method of determining distances using CaII lines works properly only inside the thin disk of the Milky Way—especially along $l = 135^\circ$, because in this particular direction the range of radial velocities caused by the galactic rotation is largest, making

Table 5: Radial velocities based on stellar HeI lines, interstellar CH lines and heliocentric distances, based on the spectroscopic parallax and galactocentric distances.

Star	Sp/L	(B-V)	RV* (km/s)	RV(CH) km/s	dist(Sp/L) (pc)	R _{gc} (kpc)
+56-574t	B1III	0.3	-36	-7	1840	9.39
+59-451b	B1II	0.69	-23	-7	2450	9.84
+59-456b	B0.5V	0.55	-49	-6	1590	9.17
+60-470t	O8V	0.70	-70	-14	2230	9.68
+60-493b	B0.5Ia	0.79	-38	-8	2790	10.16
+60-498t	O9.5V	0.53	-9	-10	2230	9.70
+60-499t	O9V	0.54	-38	-11	2830	10.19
+60-501t	O6.5V	0.45	-63	-15	3240	10.54
+60-513t	O7.5	0.49	-85	-14	2540	9.96
+60-526t	B2III	0.64	-34	-8	1090	8.81
+60-594b	O9V	0.36	-102	-14	2310	9.82
+61-411t	O8	1.00	-42	-21	4020	11.17
+61-468t	B2III	0.23	-47	-7	3060	10.41
2905t	B1Ia	0.14	0	-20	1020	8.57
5394t	B0IV	-0.15	0	0	240	8.13
12323t	O9V	-0.02	-72	-16	3700	10.85
13256b	B1Ia	1.17	-47	-54	1840	9.35
13267t	B5Ia	0.33	—	—	2580	9.95
13716t	B0.5III	0.31	-47	-2	1820	9.35
13758t	B1V	0.32	-83	-3	1310	8.97
13831t	B0III	0.10	-62	-32	2910	10.24
13841t	B2Ib	0.25	-45	-16	2330	9.77
13854t	B1Iab	0.28	-32	-6	1860	9.39
13866t	B2Ib	0.17	-51	-12	2710	10.08
13890t	B1III	0.19	-45	-17	2150	9.62
13969t	B1IV	0.31	-65	-15	1580	9.17
14014t	B0.5V	0.14	-45	-9	1720	9.28
14053t	B1II	0.25	-45	-19	3070	10.38
14134t	B3Ia	0.45	-30	-13	2210	9.68
14143t	B2Ia	0.50	-51	-10	2010	9.52
14302t	B1II-III	0.26	-44	-44	2560	9.97
14357t	B1.5II	0.32	-39	-11	2630	10.03
14434t	O6.5	0.16	-90	-19	2980	10.33
14442t	O6e	0.41	—	—	3120	10.41
14443t	B2Ib	0.34	-37	-4	2750	10.13
14476t	B0.5III	0.38	-38	-4	2080	9.58
14818t	B2Ia	0.30	-50	-13	2220	9.71
14947t	O5.5f	0.46	-46	-10	3010	10.35
15558t	O5f	0.50	-85	-7	2740	10.11
15570t	O4If	0.68	-44	-6	2310	9.77
15629t	O5Vf	0.42	-40	-10	3370	10.64
15785b	B1Iab	0.57	-32	-4	3000	10.35
16310t	B1Ib	0.65	-53	-8	1780	9.36
16429t	O5.5Iab	0.62	-50	-5	2030	9.56
17505t	O6.5V	0.40	+25	-6	1910	9.49
17520t	O9V	0.32	-29	-7	1520	9.17
20336t	B2.5V	-0.19	-18	-1	240	8.18
25940t	B3V	-0.03	+7	+7	110	8.10
236960t	B1	0.46	-37	-8	4170	11.32
27192t	B1.5IV	-0.01	+4	+4	490	8.43

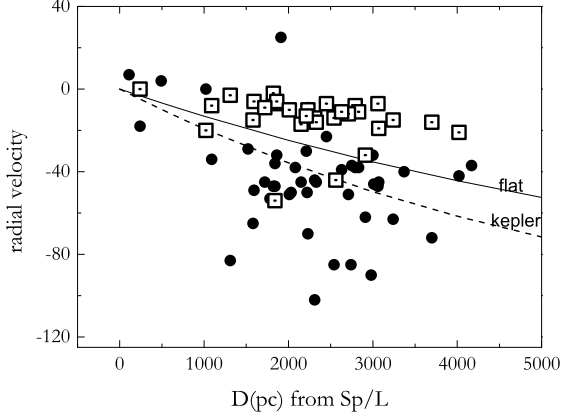


Fig. 17.— Comparison of the rotation curves based on spectrophotometric distances and radial velocities from stellar lines (filled circles) or from main CH radial components (squares)

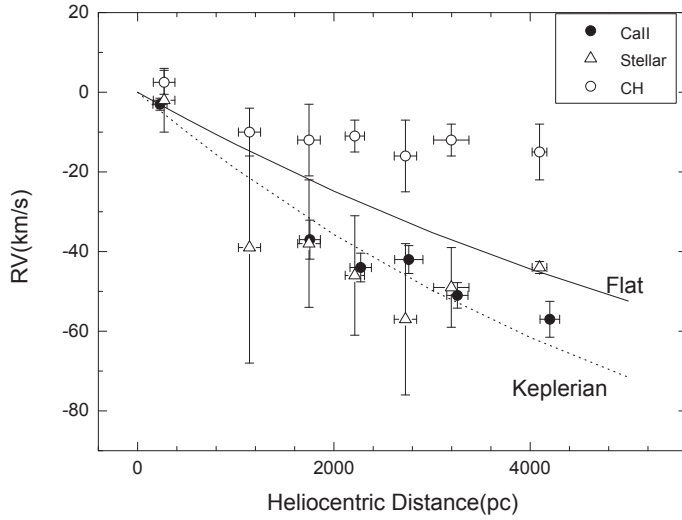


Fig. 18.— Three rotation curves using different methods, averaged in 500 pc bins. The curve based on CaII lines is mostly consistent with that based on stellar distances and radial velocities. The scatter is much greater in the latter case. The CH radial velocities may suggest orbital velocities rising outwards, because molecular clouds are usually much closer than the stars used to measure distances. The only “stellar” point that lies on the flat curve is based on only two objects. The CaII point in the 4000–4500 pc bin is also based on just two objects.

the CaII lines unsaturated even at very large distances. Higher resolution may lead to discoveries of more Doppler components and thus to larger shifts of the most blue-shifted Doppler components in the $l = 135^\circ$ direction. In that case our points in Fig. 11 could only be moved down, i.e. more strongly supporting the Keplerian rotation curve.

Moreover, it seems important to extend this method to other directions in the disk, especially at $l = 225^\circ$ (available from the Southern Hemisphere only) and to extend the galactic anticentre sample, which presently shows clearly that the radial velocities of interstellar clouds are all close to zero in relation to the LSR.

Much bigger samples of targets, observed in the chosen directions, are needed to make the conclusions well grounded, but the existing material is sufficient to conclude that the rotation curve of the thin, gaseous disc of our Galaxy is Keplerian rather than flat.

JK acknowledges the financial support of the Polish National Science Center during the period 2012–2015 (grant UMO-2011/01/BST2/05399). GAG acknowledges the support of the Chilean fund FONDECYT-regular (project 1120190). The authors acknowledge Drs. C. Moni Bidin and Boud Roukema for their valuable comments.

REFERENCES

- Bovy, J. & Tremaine, S. 2012, *ApJ*, 756, 89
- Bovy, J., Allende P., Carlos, B. et al. 2012, *ApJ*, 759, 131
- Bobylev, V.V. & Bajkova, A.T. 2011, *AstL*, 37, 526
- Brand, J. & Blitz, L. 1993, *A&A*, 275, 67
- Burgh, E. B., France, K. & McCandliss, S.R. 2007, *ApJ*, 658, 446
- Chemin, L., Carignan, C., & Foster, T. 2009, *ApJ*, 705, 1395
- Clemens, D.P. 1985, *ApJ*, 295, 422
- Corbelli, E., Lorenzoni, S., Walterbos, R., Braun, R., & Thilker, D. 2010, *A&A*, 511, A89 (C10)
- Dias, W.S., Alessi, B.S., Moitinho, A. & Lepine, J.R.D. 2002, *A&A*, 389, 871
- Georgelin, Y. M. & Georgelin, Y.P. 1976, *A&A* 49, 57
- Holmberg, J. & Flynn, C. 2000, *MNRAS*, 313, 209
- Kim, K.-M., Han, I., Valyavin, G. G., et al. 2007, *PASP*, 119, 1052
- Kharchenko, N.V., Piskunov, A.E., Roeser, S., Schilbach, E. & Scholz, R.-D. 2005, *A&A*, 438, 1163

- Kharchenko, N.V., Piskunov, A.E., Roeser, S., Schilbach, E. & Scholz, R.-D. 2005, *A&A*, 440, 403
- Kuijken, K. & Gilmore, G., 1989, *MNRAS*, 239, 651
- Liu J.C., Zhu Z., 2010, *Research in Astron. and Astrophys.*, 10, 541
- Lopez-Corredoira, M., 2014, *A&A*, 563, 128
- Lyu, C.-H., Smith, A. M., & Bruhweiler, F. C. 1994, *ApJ*, 426, 254
- Maciel, W.J., Lago, L.G., 2005, *Rev. Mex. Astr. Ap.* 41, 383
- Megier, A., Strobel, A., Bondar, A., Musaev F.A., Han Inwoo, Krelowski, J., Galazutdinov G.A. 2005, *ApJ*, 634, 451
- Megier, A., Strobel, A., Galazutdinov, J., Krelowski J. 2009, *A&A*, 507, 833
- Merrifield, M. R. 1992, *AJ*, 103, 1552
- Miyamoto, M. & Zhu, Z. 1998, *AJ*, 115, 1483
- Milgrom, A. 1983, *A&A*, 270, 365
- Moffat, A. F. J., Jackson, P. D. & Fitzgerald, M. P. 1979, *A&AS* 38, 197
- Moni Bidin, C., Carraro, J., Mendez, R.A., Smith, R. 2012, *ApJ*, 751, 30
- Oh, C. S., Kobayashi, H., Honma, M., Hirota, T., Sato, K., Ueno, Y. 2010, *PASJ*, 62, 101
- Reid, M. J., Menten, K.M., Zheng, X.W., Brunthaler, A., Moscadelli, L., Xu, Y., Zhang, B. et al. 2009, *ApJ*, 700, 137
- Sheffer, Y., Rogers, M., Federman, S. R., Lambert, D. L. & Gredel, R. 2007, *ApJ*, 667, 1002
- Sofue, Y. and Rubin, V., 2001, *Ann. Rev. Astron. Astrophys.*, 39, 137
- Schmidt-Kaler, T.: 1982, in Landolt-Boernstein, Vol. VI/2b, K. Schaifers, H.H. Voigt Eds., Springer-Verlag. 15
- Sofue, Y., Honma, M., Omodaka, T., 2009, *PASJ*, 61, 227
- Sonnentrucker, P., Welty, D. E., Thorburn, J. A. & York, D. G. 2007, *ApJS*, 168, 58
- Subramanian, A. & Bhatt, B.C. 2007, *MNRAS*, 377, 829
- Tody, D. 1993, "IRAF in the Nineties" in *Astronomical Data Analysis Software and Systems II*, A.S.P. Conference Ser., Vol 52, eds. R.J. Hanisch, R.J.V. Brissenden, & J. Barnes, 173.
- Toshihiro, O. , *AAPPS Bulletin* June 2009, 19, No. 3

Walborn, N.R. & Fitzpatrick, E.L. 1990, *PASP*, 102, 379

Welty, D.E., Hobbs, L.M. & Morton, D.C. 2003, *ApJS*, 147, 61

Xue, X. X., Rix, H. W., Zhao, G. et al. 2008, *ApJ*, 684, 1143

Zhu, Zi 2006, *Chin. J. Astr. Astrophys.* 6, 363